SIGNAL AND NOISE ANALYSIS OF DIRECT MODULATION FIBER OPTIC LINK WITH OPTICAL COMPONENT AND ARBITRARY LOSSLESS MATCHING CIRCUITS

J. A. MacDonald, E. I. Ackerman and J. L. Prince

Martin Marietta Laboratories · Syracuse
Electronics Park, Syracuse, NewYork 13221

ABSTRACT

We give a general analytical signal and noise model for a direct modulation fiber optic link that includes an optical component with gain or loss, and arbitrary lossless matching circuits at the input and output. The model equations reduce to previously published results under certain specific conditions. We describe experiments which verify various aspects of the developed model.

I. INTRODUCTION

As fiber optic links gain widespread use in radar and communications, the impact of link gain and noise becomes increasingly important. As well, links may include optical components that affect the overall signal and noise performance. A general model describing the signal and noise characteristics of a link including optical components is needed.

Cox et al. [1] derived a set of signal and noise equations for a direct modulation fiber-optic link with optimum single-frequency matching circuits at the input and output, not including detector thermal noise.

In this paper, we derive a model for the gain and noise power of a direct modulation fiber optic link using lossless (reactive) networks at the laser input and detector output. The model includes an optical processing component of gain G_o and noise figure F_o, and also includes the thermal noise contributions of the detector, which are likely to swamp the laser relative intensity noise (RIN) and detector shot noise when the optical processing component is lossy.

II. LINK EQUIVALENT CIRCUIT

Figure 1 shows the fiber optic link model used as the basis for the analysis. With the real part of input impedance Z_{in} is associated a mean square noise voltage $\langle E_{in}^2 \rangle$, where

$$\left\langle E_{in}^2 \right\rangle = 4kTBR_{in} \ . \qquad (1)$$

B is the electrical bandwidth, T is absolute temperature and k is Boltzmann's constant. R_{in} is the real part of Z_{in}. The laser impedance matching circuit is assumed to contain only reactive elements, and therefore generates no additional thermal noise. It has a current transfer function of $H_L(\omega)$ when loaded by the laser diode resistance R_L.

The input and output impedances of the laser matching circuit are given by $Z_{Li}(\omega)$ and $Z_{Lo}(\omega)$, respectively. The laser diode is modelled as an ideal diode with slope efficiency η_L in series with the junction resistance, R_L, where η_L is the ratio of optical power in the fiber, P_{opt}, to the above-threshold diode current, I_L-I_{th}. This model assumes that the laser shunt capacitance and bondwire inductance are embedded in the impedance matching network, and that the resistance in series with the shunt capacitance is negligible [2]. The laser resistance generates another thermal mean-square noise generator $\langle E_L^2 \rangle$.

The detector model consists of an ideal photodiode with junction resistance, R_j and capacitance, C_j, and series contact resistance, R_s. The two detector resistors generate mean-square noise voltages $\langle E_j^2 \rangle$ and $\langle E_s^2 \rangle$. The current induced in the diode junction, i_j is proportional to the incident photointensity by the detector responsivity, η_D. The detector

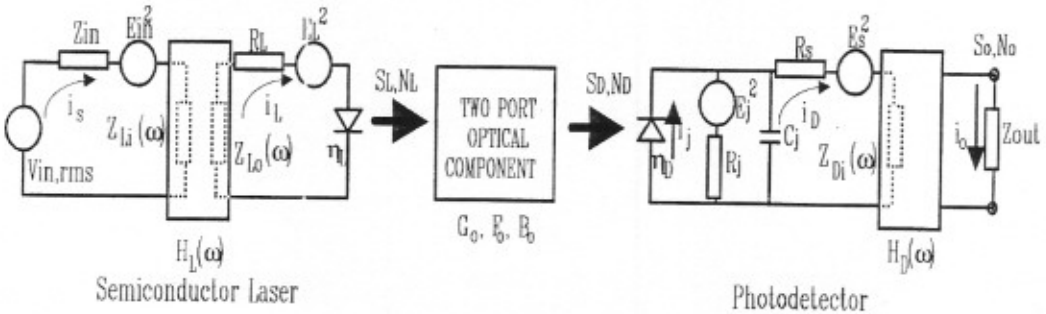

Figure 1. Link model including two-port optical component. $H_L(\omega)$ and $H_D(\omega)$ are loaded current transfer functions.

matching network has loaded current transfer function, $H_D(\omega)$ with input impedance, $Z_{Di}(\omega)$.

III. SIGNAL ANALYSIS

The available signal power at the laser input is equal to $|V_{in}(\omega)|^2/4R_{in}$. This will induce a signal current through the laser junction

$$i_L(\omega) = i_s(\omega)H_L(\omega) = \frac{V_{in}(\omega)H_L(\omega)}{Z_{in}(\omega)+Z_{Li}(\omega)} . \quad (2)$$

If the modulation level is small, i.e., $i_L << I_L - I_{th}$, then the signal power launched into the fiber is related to the junction current by the efficiency η_L defined above. The rf signal power incident on the detector facet is the laser output signal power multiplied by the gain of the optical component, G_o. This signal is demodulated by the photodiode and is delivered to the load through the detector matching circuit. The link transducer gain, G_t is the ratio of power delivered to the load to available source power. Defining R_{out} as the real part of Z_{out},

$$G_t(\omega) = \frac{4\eta_L^2\eta_D^2|H_L(\omega)|^2|H_D(\omega)|^2 G_o^2|Z_{e1}(\omega)|^2 R_{in}R_{out}}{|R_s+Z_{e1}(\omega)+Z_{Di}(\omega)|^2|Z_{in}(\omega)+Z_{Li}(\omega)|^2} . \quad (3)$$

IV. NOISE ANALYSIS

A. Laser Noise

The rf noise power in the modulated laser output beam comes from the two thermal noise sources shown in Figure 1, plus the laser relative intensity noise (RIN). [3] Performing straightforward circuit analysis to add the two thermal contributions and the RIN noise yields $N_L(\omega)$, the total noise power at the laser output,

$$N_L(\omega) = \frac{\eta_L H_L(\omega)E_{in}}{Z_{in}(\omega)+Z_{Li}(\omega)} + \frac{\eta_L E_L}{R_L+Z_{Lo}(\omega)} + \eta_L(I_L-I_{th})\sqrt{RIN\cdot B} . \quad (4)$$

B. Optical Component Noise

The two-port optical component is described by its gain, G_o, noise figure, F_o and noise-equivalent optical bandwidth, B_o. Multiple sections can be cascaded to define a single gain and noise figure. The optical bandwidth should be the noise-equivalent bandwidth incident on the detector. The noise output of the optical component is the sum of the input noise contribution and the added noise, or

$$N_D(\omega) = N_L(\omega)G_o + kT_oB_oG_o(F_o-1). \quad (5)$$

C. Demodulated Noise

The noise power out of the optical component is incident on the detector, where it is converted to a junction current according to

$$i_{j1}(\omega) = \eta_D N_D(\omega) . \quad (6)$$

The total noise power delivered to the load, $N_{o1}(\omega)$, due to the junction current, $i_j(\omega)$ is given by

$$N_{o1}(\omega) = |i_{j1}(\omega)|^2|H_D(\omega)|^2 R_{out}\frac{|Z_{e1}(\omega)|^2}{|R_s+Z_{e1}(\omega)+Z_{Di}(\omega)|^2} . \quad (7)$$

This noise power is limited by the microwave bandwidth, B. Therefore, the optical noise term in equation (5) must be multiplied by the ratio of the bandwidths, B/B_o. Substituting equations (5) and (6) into (7) and simplifying using the transducer gain, $G_t(\omega)$ given in equation (3) and the input mean-square noise voltage, $\langle E_{in}^2\rangle$ given in equation (1), the noise power delivered to the load due to the demodulated input noise becomes

$$N_{o1}(\omega) = kT_oBG_t(\omega) + \frac{kTBG_t(\omega)R_LT_L(\omega)}{|R_L+Z_{Lo}(\omega)|^2|H_L(\omega)|^2R_{in}} + \frac{(I_L-I_{th})^2RIN\cdot BG_t(\omega)T_L(\omega)}{4R_{in}|H_L(\omega)|^2} + \frac{(kT_o)^2B_oB(F_o-1)^2G_t(\omega)T_L(\omega)}{4R_{in}\eta_L^2|H_L(\omega)|^2} \quad (8)$$

where we define

$$T_L(\omega) = |Z_{in}(\omega)+Z_{Li}(\omega)|^2 \quad \Omega^2. \quad (9)$$

D. Shot Noise

A mean-square noise current is induced in the detector junction due to the random arrival of the charges associated with the dc photocurrent and demodulated signal and noise currents, all of which are uncorrelated. From the small-signal assumption made in Section II we know that the signal power is much less than the quiescent optical power. As well, the only term of equation (5) which could add significantly to the detector current is the optical component noise term. Solving for the current delivered to the load, and simplifying using the transducer gain, the power due to shot noise delivered to the load, $N_{o2}(\omega)$ in the microwave bandwidth, B becomes

$$N_{o2}(\omega) = \frac{qBT_L(\omega)G_t(\omega)}{2\eta_L^2\eta_DG_o|H_L(\omega)|^2R_{in}}\left[\eta_L(I_L-I_{th})+kT_oB_o(F_o-1)\right] . \quad (10)$$

E. Detector Thermal Noise

As shown in Figure 1, the two detector resistances generate mean-square thermal noise voltages given by $\langle E_j^2\rangle$ and $\langle E_s^2\rangle$. Performing the circuit analysis, the noise power delivered to the load, $N_{o3}(\omega)$ is given by

$$N_{o3}(\omega) = \frac{4kTB|H_D(\omega)|^2R_{out}}{|R_s+Z_{e1}(\omega)+Z_{Di}(\omega)|^2}\left[\frac{|Z_{e1}(\omega)|^2}{R_j}+R_s\right] = \frac{kTBG_t(\omega)T_L(\omega)}{\eta_L^2\eta_D^2G_o^2|H_L(\omega)|^2R_{in}}\left[\frac{1}{R_j}+\frac{R_s}{R_j^2}+\omega^2C_j^2R_s\right] . \quad (11)$$

F. Output Noise Power

The total noise power, $N_o(\omega)$ delivered to the load is the sum of the demodulated noise given in equation (8), the shot noise (10) and the thermal noise (11),

$$N_o(\omega) = kT_oBG_t(\omega) + \frac{kTBG_t(\omega)R_LT_L(\omega)}{|R_L + Z_{Lo}(\omega)|^2 |H_L(\omega)|^2 R_{in}}$$
$$+ \frac{(I_L - I_{th})^2 RIN \cdot BG_t(\omega)T_L(\omega)}{4R_{in}|H_L(\omega)|^2}$$
$$+ \frac{(kT_o)^2 B_oB(F_0 - 1)^2 G_t(\omega)T_L(\omega)}{4R_{in}\eta_L^2|H_L(\omega)|^2}$$
$$+ \frac{qBT_L(\omega)G_t(\omega)}{2\eta_L^2\eta_D G_o|H_L(\omega)|^2 R_{in}}\left[\eta_L(I_L - I_{th}) + kT_oB_o(F_0 - 1)\right]$$
$$+ \frac{kTBG_t(\omega)T_L(\omega)}{\eta_L^2\eta_D^2 G_o^2|H_L(\omega)|^2 R_{in}}\left[\frac{1}{R_j} + \frac{R_s}{R_j^2} + \omega^2 C_j^2 R_s\right]. \quad (12)$$

To summarize, the first two terms in equation (12) represent the noise at the output due to the thermal noise from the laser circuit. The third term represents the laser RIN noise. The fourth term is the noise due to the optical component. Fifth is the shot noise term, and last is the detector thermal noise term.

V. EXPERIMENTAL VERIFICATION OF MODEL

A. Signal and Noise Relationships

For narrowband signals, an optimum single frequency match at the input and output will typically suffice. If we consider the additional condition that $Z_{in} = Z_{out} = Z_o$, then

$$|H_L(\omega)|^2 = \frac{Z_o}{R_L} \quad \text{and} \quad |H_D(\omega)|^2 = \frac{R_s}{Z_o}. \quad (13)$$

Solving the circuit, the matched transducer gain, $G_{tm}(\omega)$ becomes

$$G_{tm}(\omega) = \frac{\eta_L^2\eta_D^2 G_o^2 R_s R_j^2}{4R_L(1 + \omega^2 R_j^2 C_j^2)\left[R_s + \frac{R_j}{1 + \omega^2 R_j^2 C_j^2}\right]^2}. \quad (14)$$

For many applications the junction resistance is large enough to ignore, and equation (14) reduces to

$$\lim_{R_j \to \infty} G_{tm}(\omega) = \frac{\eta_L^2\eta_D^2 G_o^2}{4\omega^2 C_j^2 R_s R_L}, \quad (15)$$

which agrees with the results of Kasemset et al. [4] Again using the ideal match conditions, the output noise power, $N_{om}(\omega)$ becomes

$$N_{om}(\omega) = 2kTBG_{tm}(\omega) + (I_L - I_{th})^2 RIN \cdot BG_{tm}(\omega)R_L$$
$$+ \frac{(kT_o)^2 B_oB(F_0 - 1)^2 G_t(\omega)R_L}{\eta_L^2}$$
$$+ \frac{2qBG_{tm}(\omega)R_L}{\eta_L^2\eta_D G_o}\left[\eta_L(I_L - I_{th}) + kT_oB_o(F_0 - 1)\right]. \quad (16)$$
$$+ \frac{4kTBG_{tm}(\omega)R_L}{\eta_L^2\eta_D^2 G_o^2}\left[\frac{1}{R_j} + \frac{R_s}{R_j^2} + \omega^2 C_j^2 R_s\right]$$

B. Noise Figure

The noise figure of the link is, by definition,

$$F \equiv \frac{N_{out}}{kT_oBG_{av}} \quad (17)$$

where T_o is 290°K, N_{out} is the available output noise power when the input terminals are at T_o, and G_{av} is the available gain. If the input and output are ideally matched at a single frequency, then the transducer gain, G_{tm} is equivalent to the available gain, G_{av}. Therefore, the noise figure of the ideally matched link can be calculated using N_{om} from equation (16) and G_{tm}, given in (14). Also, if the detector junction resistance is large enough to ignore, the noise figure is found to agree with the results of Cox et al. [1], with the addition of the optical component term and the detector thermal noise term ($1/G_{tm}$),

$$\lim_{R_j \to \infty} F = 2 + \frac{(I_L - I_{th})^2 RIN \cdot R_L}{kT_o} + \frac{kTB_o(F_0 - 1)^2 R_L}{\eta_L^2}$$
$$+ \frac{2qR_L}{kT_o\eta_L^2\eta_D G_o}\left[\eta_L(I_L - I_{th}) + kT_oB_o(F_o - 1)\right] + \frac{1}{G_{tm}} \quad (18)$$

C. Experimental Verification Using Optimum Match

For our first experiment, measurements were taken on the circuit shown in Figure 1, with both the laser and detector tuned to an optimum match at 10GHz. The optical component was an attenuator. The predicted noise power, gain and signal-to-noise ratio were plotted against the optical gain, along with the measured results, in Figure 2. The plots show excellent correlation. The flat SNR region is the RIN-limited case, and the slope of 2 in the SNR is the region where the link is at the thermal noise floor.

The maximum link gain was -4.7dB, occurring when the optical loss was minimum (0.5dB, due to an optical splice connector). This is close to the record 10GHz result (-3.3dB) that we achieved previously using a similar link. [5]

D. Untuned Laser/Detector Model

We performed a second experiment, in which the rf connections into the laser and out of the detector were made via 50Ω microstrip transmission lines. Under these conditions, the model equations can be reduced by applying the lossless transmission line equation. At 6GHz, the gain and output noise power were measured as the attenuator was varied. Measured and modelled performance track very closely, as shown in Figure 3 below.

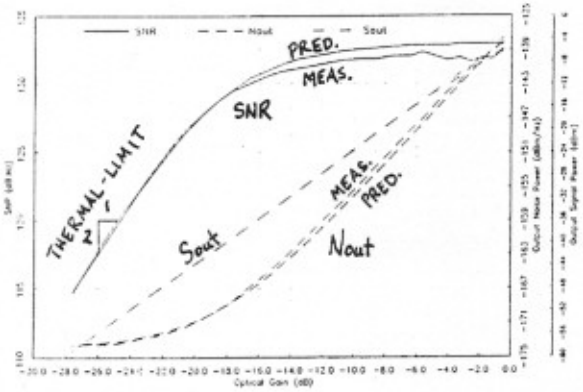

Figure 2. Measured and predicted results of signal power, noise power and signal-to-noise ratio for experimental link at 10GHz, with P_{in}=0dBm.

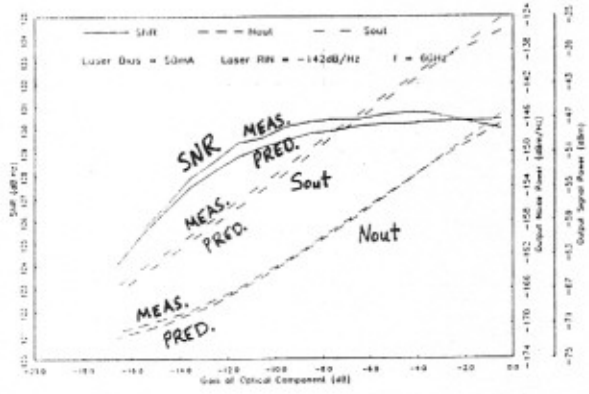

Figure 3. Measured and predicted results of signal power, noise power and signal-to-noise ratio for untuned link at 6GHz, with P_{in}=0dBm.

VI. OPTICAL AMPLIFIER CONSIDERATIONS

A. Use of Optical Amplifiers to Improve SNR

Some photonic systems employ various stages of lossy optical signal processing. Because semiconductor lasers are noisy, including lossy components in the optical chain can significantly worsen the link SNR. One way to improve SNR is to reduce the optical loss of the processing component by including an optical amplifier. An optical filter should also be used at the output of the amp to reduce the optical bandwidth. If this is not done, the optical component noise term of equation (12) may dominate, resulting in a very high output noise floor.

B. Experimental Verification Using an Optical Amplifier

The fourth term of equation (12) arises from the noise added by the optical component. If F_o and B_o are large, the minimum output noise floor can be limited by this term. To verify this, we performed a third experiment using the untuned link described in section V, with a semiconductor optical amplifier at the output of the attenuator. Using an optical spectrum analyzer, we measured the gain, noise figure and noise-equivalent bandwidth of this amp at three different bias levels. In order to maintain the large noise bandwidth and verify the model equations, we did not put a filter at the output of the amp. We then measured the output noise floor of the link with 30dB of attenuation, and compared these measurements to the model predictions. Table 1 shows these results. The measured output noise powers are within 2dB of the expected values. The noise floor is above the thermal limit of -174 dBm/Hz, which highlights the need for an optical filter at the output of an amplifier with large amplified spontaneous emission noise.

Amp Bias (mA)	G_a (dB)	F_a (dB)	B_o (GHz)	$N_{o,expect}$ (dBm/Hz)	$N_{o,meas}$ (dBm/Hz)
40	5	23	8000	-172	-170
60	10	25	8000	-163	-162
80	13	27	8000	-154	-156

Table 1. Expected and measured output noise floors at 6GHz for untuned link with an optical amp. G_a and F_a are gain and noise figure of amplifier alone.

This work was supported by the U.S. Army Space and Strategic Defense Command, Huntsville, Alabama.

REFERENCES

[1] Cox, C. H., L. M. Johnson, and G. E. Betts, "A Theoretical and Experimental Comparison of Directly and Externally Modulated Fiber-Optic Links," 1989 MTT-S Symposium Digest, vol. II, pp. 689-692.

[2] Tucker, R. S., and D. J. Pope, "Microwave Circuit Models of Semiconductor Injection Lasers," IEEE Trans. Micr. Theory Tech., vol. 31, No. 3, March 1983, pp. 289-294.

[3] Lau, K. Y., and A. Yariv, "Ultra-High Speed Semiconductor Lasers," IEEE J. Quantum Electron., vol. QE-21, No. 2, February, 1985, pp. 121-137.

[4] Kasemset, D., E. Ackerman, S. Wanuga, P. Herczfeld, and A. Daryoush, "A Comparison of Alternative Modulation Techniques for Microwave Optical Links," Proc. SPIE, vol. 1371, pp. 104-114.

[5] Prince, J., J. MacDonald, and E. Ackerman, "Low-Loss X-Band Direct Modulation Fiber Optic Link," ARPA Symp. on Photonic Systems for Ant. Appl., Jan. 18-21, 1994.